Vomocytosis of live pathogens from macrophages is regulated by the atypical MAP kinase ERK5

Gilbert, Andrew S.; Seoane, Paula I.; Sephton-Clark, Poppy; Bojarczuk, Aleksandra; Hotham, Richard; Giurisato, Emanuele; Sarhan, Adil R.; Hillen, Amy; Velde, Greetje Vande; Gray, Nathanael S.; Alessi, Dario; Cunningham, Debbie L.; Tournier, Cathy; Johnston, Simon A.; May, Robin C.

Published in:
Science Advances

DOI:
10.1126/sciadv.1700898

Publication date:
2017

Document Version
Publisher's PDF, also known as Version of record

IMMUNOLOGY

Vomocytosis of live pathogens from macrophages is regulated by the atypical MAP kinase ERK5

Andrew S. Gilbert,[1] Paula I. Seoane,[1] Poppy Sephton-Clark,[1] Aleksandra Bojarczuk,[2,3] Richard Hotham,[2,3] Emanuele Giurisato,[4,5] Adil R. Sarhan,[1,6] Amy Hillen,[7] Greetje Vande Velde,[7] Nathanael S. Gray,[8,9] Dario R. Alessi,[6] Debbie L. Cunningham,[1] Cathy Tournier,[4] Simon A. Johnston,[2,3] Robin C. May[1]*

Vomocytosis, or nonlytic extrusion, is a poorly understood process through which macrophages release live pathogens that they have failed to kill back into the extracellular environment. Vomocytosis is conserved across vertebrates and occurs with a diverse range of pathogens, but to date, the host signaling events that underpin expulsion remain entirely unknown. We use a targeted inhibitor screen to identify the MAP kinase ERK5 as a critical suppressor of vomocytosis. Pharmacological inhibition or genetic manipulation of ERK5 activity significantly raises vomocytosis rates in human macrophages, whereas stimulation of the ERK5 signaling pathway inhibits vomocytosis. Lastly, using a zebrafish model of cryptococcal disease, we show that reducing ERK5 activity in vivo stimulates vomocytosis and results in reduced dissemination of infection. ERK5 therefore represents the first host signaling regulator of vomocytosis to be identified and a potential target for the future development of vomocytosis-modulating therapies.

INTRODUCTION

Phagocytes are an essential component of the innate immune system, which function to identify, engulf, and destroy foreign particles. Although the vast majority of microbes are readily killed by phagocytes upon internalization, a number of important human pathogens have evolved mechanisms to survive or replicate within this hostile host environment. Phagocytes infected with these organisms have one of two fates: either they successfully recognize and destroy the intracellular pathogen or the pathogen lyses and kills the host cell. More than 10 years ago, we and others discovered a third potential outcome, whereby host macrophages expel the live pathogen residing within it in a process known as vomocytosis or nonlytic extrusion (*1*, *2*). Vomocytosis has subsequently been observed with a diverse range of pathogens (*3*) and in phagocytic cells from mammals (*4*), birds (*5*), fish (*6*), and amoebae (*7*), suggesting that it is an evolutionarily conserved phenomenon. However, despite this marked conservation, the host molecules that regulate vomocytosis have remained enigmatic.

RESULTS

To begin addressing the underlying molecular pathways that regulate vomocytosis, we screened a library of inhibitors that target kinases known to be expressed in macrophages (table S1) (*8*). This initial screen identified one compound [LRRK2-IN-1 (*9*)] that showed a small but significant increase in vomocytosis rates without enhancing cell death. LRRK2-IN-1 inhibits the leucine-rich repeat kinase LRRK2 but has additionally been demonstrated to act against other kinases, including the bromodomain protein BRD4 (*10*) and the extracellular receptor kinase 5 (ERK5) (*11*). Testing an independent second series of inhibitors revealed a potent and reproducible enhancement of vomocytosis with the ERK5 inhibitors XMD17-109 (*12*) or AX15836, but not with a specific inhibitor of BRD4 [JQ1 (*13*)] or with an alternative inhibitor of LRRK2 [HG1010201 (*14*)] (Fig. 1A and table S1). Notably, direct exposure of cryptococci to ERK5 inhibitors in vitro did not alter fungal morphology or growth rate (fig. S1), indicating that the impact of ERK5 inhibition on vomocytosis acts at the level of the host macrophage and not of the pathogen itself. In addition, exposing cells to LRRK2-IN-1 and XMD17-109 together did not enhance vomocytosis levels beyond that of XMD17-109 alone, suggesting that it is the off-target inhibition of ERK5 by LRRK2-IN-1 that accounts for its effect on vomocytosis.

To confirm this role for ERK5 in enhancing vomocytosis, we first exposed human macrophages, differentiated from peripheral blood monocytes, to XMD17-109. It has previously been shown that primary human macrophages show higher basal rates of vomocytosis than phagocytic cell lines (*2*), but nevertheless, as with J774 cells (which are originally derived from mouse), human macrophages showed a significant increase in vomocytosis when ERK5 activity was inhibited (Fig. 1B). Second, we tested the role of ERK5 in vomocytosis directly by depleting ERK5 levels in macrophages using transient small interfering RNA (siRNA)–based knockdown in J774 cells (Fig. 1C) or tamoxifen-inducible *ERK5* gene loss in murine bone marrow–derived macrophages (Fig. 1D). In both cases, we were unable to achieve full loss of the ERK5 protein (fig. S2), but this partial reduction in ERK5 level nevertheless resulted in a reproducible enhancement of vomocytosis. Thus, either pharmacological inhibition or genetic removal of ERK5 enhances vomocytosis in vitro.

Vomocytosis has been reported to occur with a wide range of live phagocytic targets but has never been observed with inert particles or dead pathogens. In line with this observation, pharmacological inhibition of ERK5 similarly enhanced vomocytosis of a second fungal

[1]Institute of Microbiology and Infection, School of Biosciences, University of Birmingham, Edgbaston, Birmingham B15 2TT, UK. [2]Department of Infection, Immunity and Cardiovascular Disease, Medical School, University of Sheffield, Sheffield, UK. [3]Bateson Centre, University of Sheffield, Sheffield, UK. [4]Division of Molecular and Clinical Cancer, School of Medical Sciences, Faculty of Biology, Medicine and Health, University of Manchester, Manchester M13 9PT, UK. [5]Department of Molecular and Developmental Medicine, University of Siena, 53100 Siena, Italy. [6]Medical Research Council Protein Phosphorylation and Ubiquitylation Unit, College of Life Sciences, University of Dundee, Dow Street, Dundee DD1 5EH, Scotland. [7]Biomedical MRI/MoSAIC, Department of Imaging and Pathology, KU Leuven–University of Leuven, Leuven, Belgium. [8]Department of Cancer Biology, Dana-Farber Cancer Institute, Boston, MA 02115, USA. [9]Department of Biological Chemistry and Molecular Pharmacology, Harvard Medical School, 250 Longwood Avenue, SGM 628, Boston, MA 02115, USA.
*Corresponding author. Email: r.c.may@bham.ac.uk

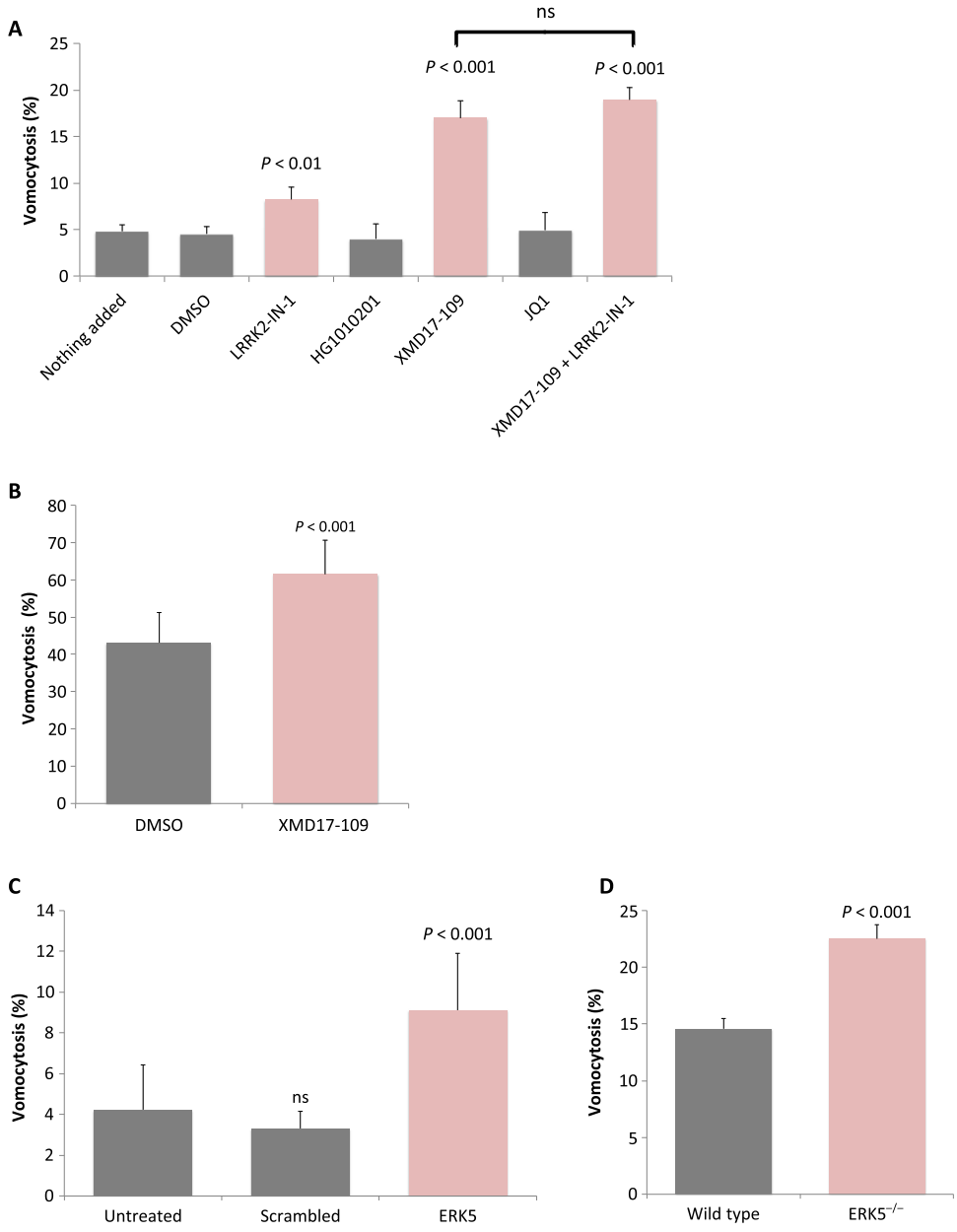

Fig. 1. Pharmacological or genetic inhibition of ERK5 enhances vomocytosis in vitro and ex vivo. (**A**) Vomocytosis is enhanced in J774.A1 cells by the LRRK2 inhibitor LRRK2-IN-1 (1 μM) but not by a second LRRK2 inhibitor, HG1010201 (1 μM). Vomocytosis is more strongly enhanced by specific inhibition of ERK5 (an off-target of LRRK2-IN-1) by XMD17-109 (1 μM) but not by inhibition of a second off-target, BRD4, by the inhibitor JQ1 (1 μM). Dual application of LRRK2-IN-1 and XMD17-109 (1 μM of each) showed significant enhancement of vomocytosis that was not significantly different to that of XMD17-109 alone. ns, not significant. (**B**) Application of 1 μM XMD17-109 to human PBMC-derived macrophages also significantly enhances vomocytosis rates in vitro. (**C**) Partial knockdown of ERK5 expression in J774.A1 by siRNA enhances vomocytosis. (**D**) Tamoxifen-inducible reduction of ERK5 expression ex vivo in murine bone marrow–derived macrophages significantly raises vomocytosis rates. Statistical significance was tested by χ^2 using a Bonferroni correction for multiplicity. All data represent pooled, averaged data from three to nine experimental repeats, with error bars showing the SEM. Example movies used for scoring are shown in movies S1 and S2.

pathogen, *Cryptococcus gattii*, but despite extensive imaging we were not able to observe any expulsion events for latex beads or heat-inactivated cryptococci (Fig. 2A). Thus, ERK5 is acting as a suppressor of the canonical vomocytosis pathway, rather than artificially inducing expulsion of all phagocytic cargo.

The canonical ERK5 pathway involves ERK5 activation via the upstream mitogen-activated protein (MAP) kinase MEK5 (*15*). Inhibition of MEK5 with the specific inhibitor BIX02189 (*16*) similarly raised vomocytosis levels in macrophages (Fig. 2B), suggesting that vomocytosis rates are normally suppressed by the MEK5-ERK5 signaling axis. To test this possibility further, we exposed cells to insulin-like growth factor 2 (IGF2), which has previously been shown to activate MEK5-ERK5 signaling up to eightfold (*17*) and to be implicated in phagocyte behavior (*18*). In line with this, IGF2 stimulation reduced cryptococcal

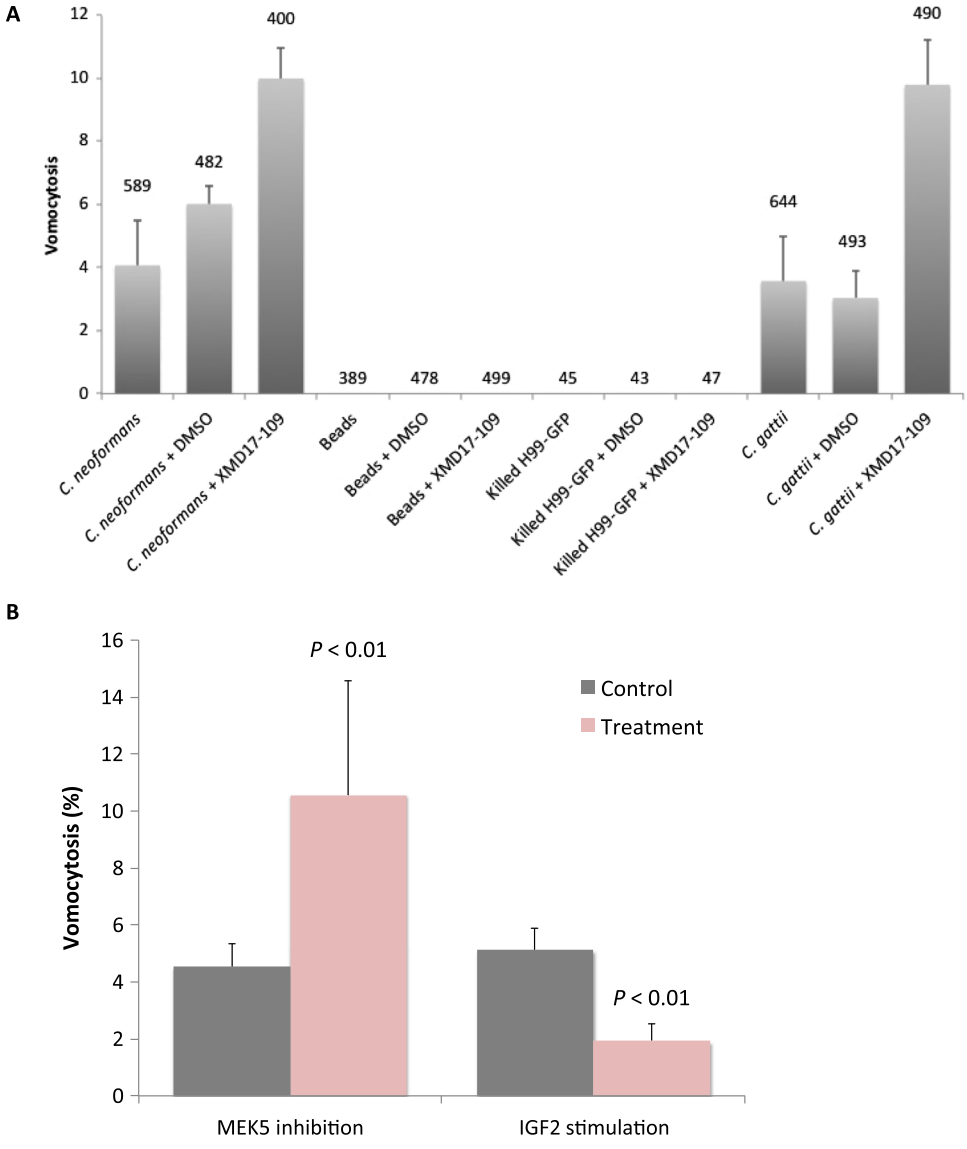

Fig. 2. Modulation of the canonical ERK5 signaling pathway alters vomocytosis rate but does not induce expulsion of inert phagosomal cargo. (**A**) ERK5 inhibition enhances vomocytosis of both *C. neoformans* and *C. gattii* but does not induce vomocytosis of heat-killed cryptococci or inert 3-μm polycarbonate beads. Numbers above each column represent the total number of individual fungal cells or beads scored. (**B**) Inhibition of MEK5 activity (an upstream regulator of ERK5) with 3 μM BIX02189 recapitulates the enhancement of vomocytosis seen with ERK5 inhibition in J774 macrophages, whereas stimulation of the ERK5 pathway via 1 μM IGF2 significantly reduces vomocytosis rates. Statistical significance was tested by χ^2 on raw data from three independent repeats. Error bars represent the SEM.

expulsion rates from macrophages (Fig. 2B). Thus, pharmacological or genetic inhibition of the ERK5 pathway enhances vomocytosis, and indirect stimulation of the pathway via IGF2 suppresses it.

Macrophage behavior is strongly influenced by the local concentration of cytokines, released both by themselves and by other cell types. In particular, different cytokine environments can modulate macrophage activation states (*19*), and we and others have previously shown that altered macrophage polarization states modify vomocytosis rates (*20*). We therefore considered whether ERK5 might regulate vomocytosis by modifying macrophage polarization and the local cytokine environment.

To determine the impact of ERK5 on macrophage polarization, we assessed the expression of surface markers on J774 macrophages exposed to XMD17-109. At rest, macrophages express both the pro-inflammatory marker CD86 and the anti-inflammatory marker MGL but are efficiently polarized to $CD86^{hi}$ (M1-like) cells when exposed to exogenous interferon-γ (IFN-γ) and lipopolysaccharide (LPS) or conversely to MGL^{hi} (M2-like) cells upon exposure to interleukin-4 (IL-4) (Fig. 3A). Cells treated with XMD17-109 showed no change in the expression of CD86 markers (Fig. 3A, i) either at rest or stimulated with IFN-γ and LPS. In contrast, XMD17-109 treatment strongly reduced the expression of MGL both in resting cells and in cells polarized by exposure to IL-4 (Fig. 3A, ii). Thus, ERK5 inhibition in macrophages leads to a modified inflammatory profile that prevents anti-inflammatory polarization without modifying their response to inflammatory stimuli.

To determine the consequence of this modified inflammatory profile, we performed enzyme-linked immunosorbent assay (ELISA) analysis to quantify secreted cytokine levels in supernatants from mouse

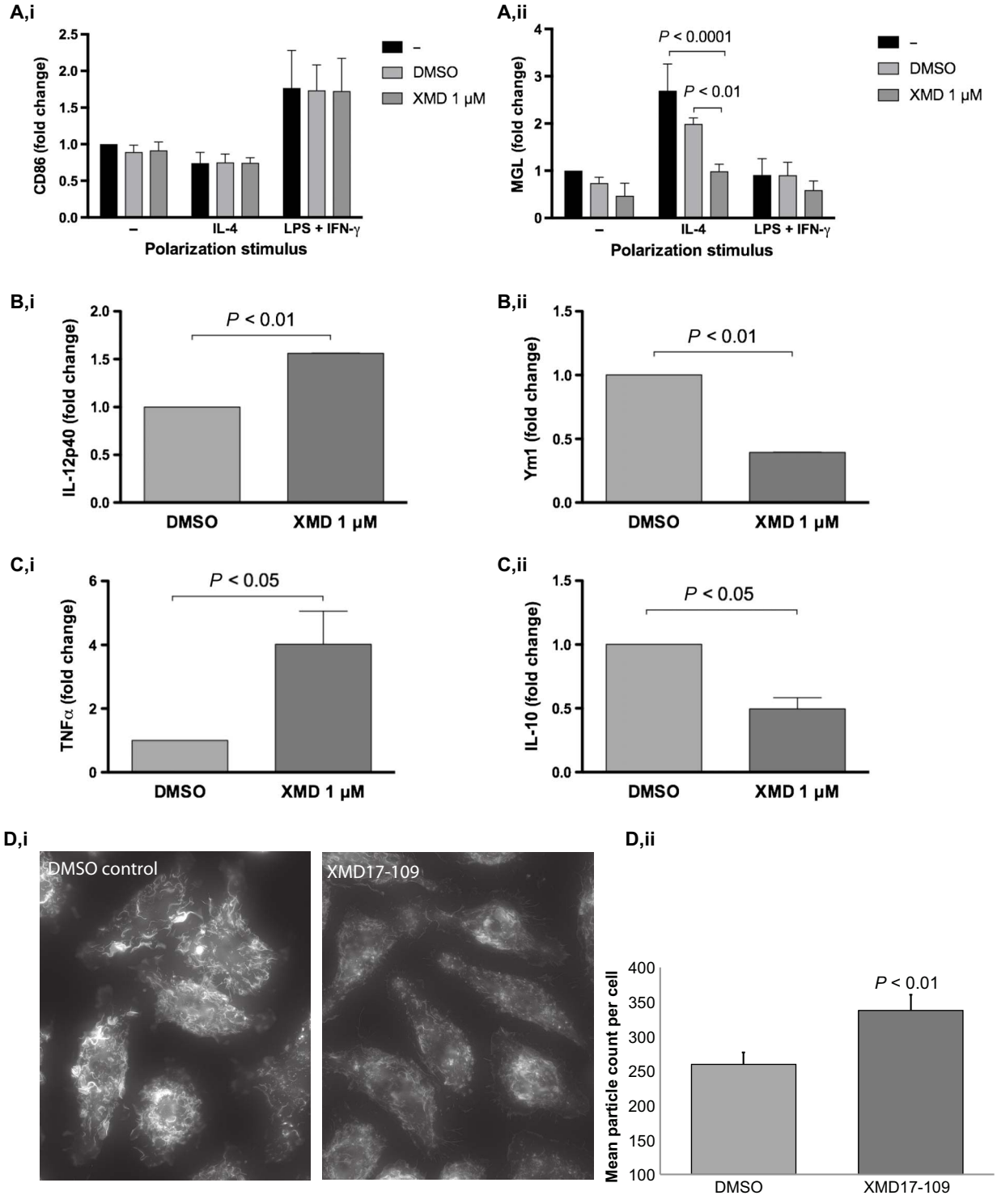

Fig. 3. ERK5 inhibition suppresses M2 macrophage polarization, alters secreted cytokine profiles, and modifies the actin cytoskeleton. (**A**) (i) Pharmacological inhibition of ERK5 with XMD17-109 does not alter expression of the M1 macrophage marker CD86 in J774 macrophages at rest or under M1 (LPS and IFN-γ) or M2 (IL-4) stimulating conditions. (ii) However, IL-4–driven M2 polarization is strongly reduced in the presence of XMD17-109. Significance was tested using two-way analysis of variance (ANOVA) on data from three independent replicates. Error bars show the SEM. (**B**) XMD17-109 inhibition of ERK5 activity in J774 macrophages increases proinflammatory IL-12p40 secretion (i) while reducing the secretion of the M2 marker Ym1 (ii). Significance was tested using a ratio-paired *t* test. (**C**) XMD17-109 inhibition of ERK5 activity in human PBMC-derived macrophages increases proinflammatory TNFα secretion (i) while reducing the secretion of the anti-inflammatory cytokine IL-10 (ii). Significance was tested using a ratio-paired *t* test. (**D**) J774 macrophages treated with XMD17-109 show a reduction in actin ruffles (revealed using Alexa 488–phalloidin; i). (ii) Ruffle disruption by XMD17-109 results in increased numbers of smaller actin-rich fragments, quantified in binary images (n = 33 images from n = 3 replicates, two-tailed *t* test; error bars are SEM). Images were captured using identical illumination, exposure, and postacquisition processing settings.

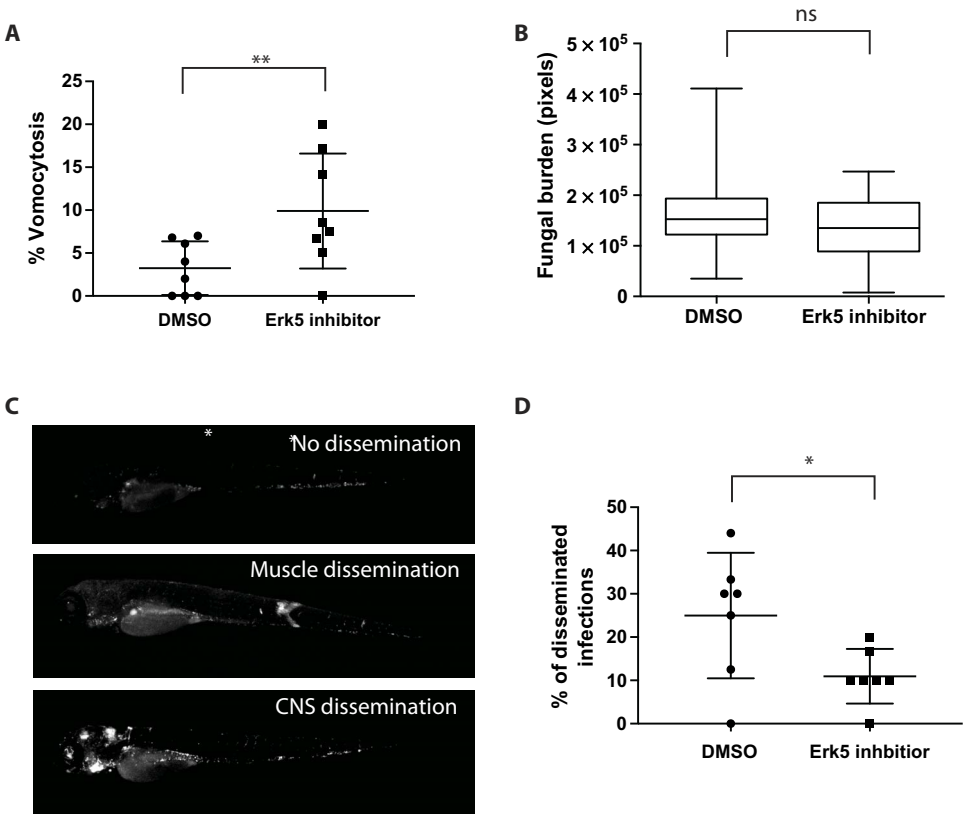

Fig. 4. ERK5 inhibition enhances vomocytosis and reduces dissemination in a zebrafish model of cryptococcosis. (**A**) Infected zebrafish treated with XMD17-109 show a significant ($P = 0.001$, Fisher's exact test) increase in vomocytosis in vivo over 24 hours. Bars represent the median and 5th/95th percentile. (**B**) Overall fungal burden at 3 days after infection is not significantly altered by ERK5 inhibition. Bars represent the median and 5th/95th percentile, with the boxed region representing the interquartile range. (**C**) Individual infections can be individually scored as nondisseminated (restricted to the bloodstream; top), disseminated to muscle/tissue blocks (middle), or disseminated to the central nervous system (bottom). CNS, central nervous system. (**D**) Infected fish treated with XMD17-109 show significantly ($P < 0.05$, Fisher's exact test) reduced dissemination from the site of infection. Bars represent the median and 5th/95th percentile.

macrophages (Fig. 3B) and human monocyte-derived macrophages (Fig. 3C) treated with XMD17-109. In line with the reduction in IL-4 polarization induced by ERK5 inhibition, both cell types showed an increased secretion of proinflammatory cytokines [IL-12p40 or tumor necrosis factor–α (TNFα)] and a reduced secretion of M2-associated proteins (Ym1 or IL-10) upon exposure to XMD17-109.

ERK5 has previously been implicated in cytoskeletal remodeling (*21*, *22*), and previous work has shown that mild inhibition of phagocyte actin dynamics triggers enhanced vomocytosis (*23*). We therefore fixed J774 cells exposed to *C. neoformans* in the presence or absence of XMD17-109 and stained for filamentous actin. ERK5 inhibition did not lead to any gross alteration of the actin cytoskeleton, in line with our observation that XMD17-109 does not alter phagocytosis rates or cell motility (both actin-driven processes). However, we noted a subtle reduction in the number and size of actin-rich ruffles in treated cells, suggestive of a slight destabilization of actin filamentation during ERK5 inhibition (Fig. 3D). Thus, the impact of ERK5 inhibition on vomocytosis likely results from a combination of reduced M2 inflammatory signaling and a diminished ability to constrain cryptococci within filamentous actin "cages."

Vomocytosis was first observed more than a decade ago (*1*, *2*), but an enduring open question in the field has been whether it serves to increase or reduce pathogenesis in infected organisms. Although in vivo vomocytosis has been implied indirectly (*4*), it is only very recently that extended imaging in the zebrafish model has provided direct evidence for its occurrence within a living animal (*6*, *24*).

We exploited this model to explore the impact of modifying vomocytosis rates on cryptococcal disease progression. We infected zebrafish larvae in the presence of XMD17-109 or a dimethyl sulfoxide (DMSO) control and then used extended live-cell imaging of anesthetized fish to quantify vomocytosis in vivo. As with our in vitro studies, ERK5 inhibition led to significantly enhanced vomocytosis rates in vivo (Fig. 4A). However, although the overall fungal burden at day 3 after infection did not differ significantly between control and inhibitor-treated fish, ERK5 inhibition led to a significant decrease in disease dissemination from the initial point of infection (Fig. 4B). In humans, cryptococcal dissemination from the lung (the initial point of entry) to other tissues (in particular, the central nervous system) is thought to depend, at least in part, on "Trojan Horse" transportation within host phagocytes (*25*). Thus, elevating vomocytosis rates presumably reduces dissemination by triggering phagocytes to eject their fungal cargo before they migrate far from the initial site of infection.

DISCUSSION

Together, these findings identify ERK5 as the first cellular signaling component to regulate vomocytosis. There are a number of ERK5 inhibitors under clinical development (*15*), and further work is needed

to understand whether targeting vomocytosis has promising therapeutic value. However, we note that the ERK5 locus is polymorphic in humans and that specific polymorphisms have been linked to lung cancer risk in smokers (*26*) and thus variation in ERK5 activity may contribute to the significant individual variation in vomocytosis rate between healthy donors and, consequently, to the risk of disseminated cryptococcosis.

MATERIALS AND METHODS

All reagents and media were purchased from Sigma-Aldrich, unless specified otherwise.

Cryptococcus strains

Strains used were *C. neoformans* var. *grubii* serotype A wild-type strains H99 or KN99, green fluorescent protein (GFP)–expressing derivatives KN99-GFP or H99-GFP, and *C. gattii* serotype B R265 or its GFP-expressing derivative R265-GFP (*27*). These were grown overnight in yeast peptone dextrose broth (2% glucose, 1% peptone, and 1% yeast extract) at 25°C on an orbital rotator (20 rpm).

J774A.1 cell culture

J774A.1 murine macrophages were cultured at 37°C in 5% CO_2 in complete Dulbecco's modified Eagle medium (DMEM) with 2 mM L-glutamine, streptomycin (100 U/ml) and penicillin (0.1 mg/ml), and 10% fetal bovine serum (FBS) and passaged when confluent by scraping and resuspension in fresh medium.

Human primary macrophage isolation and culture

All work with human tissue was approved by the University of Birmingham Ethics Committee under reference ERN_10-0660. Twenty to forty ml of blood was withdrawn from healthy volunteers by venipuncture and diluted twice in cold phosphate-buffered saline (PBS) before layering on top of 20 ml of Ficoll-Paque. Samples were centrifuged at 400*g* for 30 min at 20°C without braking in a swing bucket rotor. The white disc of peripheral blood mononuclear cells (PBMCs) obtained was washed twice in cold PBS (harvesting cells in between by centrifugation at 300*g* for 10 min), resuspended in PBS, counted, and then plated onto multiwell dishes in RPMI 1640 with 10% FBS and granulocyte-macrophage colony-stimulating factor (50 ng/ml).

Murine bone marrow–derived macrophage isolation and culture

Mice carrying the *erk5F* allele and the CMV-CreER transgenes were identified by polymerase chain reaction (PCR) on genomic DNA, as previously described (*28*). The colony was maintained in a pathogen-free facility at the University of Manchester, and all animal procedures were performed under license in accordance with the UK Home Office Animals (Scientific Procedures) Act 1986 and institutional guidelines. Primary macrophages were obtained from bone marrow cells isolated from femurs of genetically modified mice and cultured in DMEM containing 10% FBS, 1% penicillin/streptomycin, and 20% L929 cell-conditioned medium as a source of CSF-1 (colony-stimulating factor–1). Where indicated, the cells were mock-treated with DMSO or incubated with 4-hydroxytamoxifen (4-HT; 0.1 μM) at day 5 to induce Cre-mediated recombination of the *erk5F* allele.

In vitro infection and imaging

Fungi were opsonized with pooled human AB serum for 1 hour at 37°C and 5% CO_2 before infection. Macrophages were exposed to fungal cells at a multiplicity of infection of 10:1 for 2 hours, with or without the addition of inhibitors or DMSO controls. Extracellular fungi were removed by washing with fresh medium, containing inhibitors or DMSO control, and maintained under these conditions for 18 hours of time-lapse imaging. Time-lapse movies were made using a Ti-E Nikon or Zeiss Axio Observer microscope. Samples were incubated at 37°C and 5% CO_2 in the microscope imaging chamber. Images were taken every 5 min for 18 hours and compiled into single movie files for analysis using NIS Elements or Zeiss Zen software, respectively. Movies were blinded by a third party before manual scoring for vomocytosis and macrophage integrity. Vomocytosis was scored visually using the following preagreed guidelines:

(1) One vomocytosis event is the expulsion of internalized cryptococci from an infected macrophage, regardless of the number of cryptococci expelled if they do so simultaneously.

(2) Vomocytosis events are scored as independent phenomena if they occur in different frames or from different macrophages.

(3) Vomocytosis events are discounted if the host macrophage subsequently undergoes lysis or apoptosis within 30 min.

For fixed cell imaging, cells were plated onto glass coverslips and then infected as above before fixing with 4% paraformaldehyde in PBS (10 min) and then staining with Alexa 488–phalloidin (20 min). Coverslips were mounted onto glass slides using ProLong Antifade and imaged on a Zeiss Axio Observer.

ERK5 siRNA

Accell Mouse MAPK7 (ERK5)–SMARTpool siRNA was purchased from Dharmacon GE Healthcare and used according to the manufacturer's instructions. J774A.1 murine macrophages (5.0×10^3) were seeded into a 96-well plate and incubated at 37°C and 5% CO_2 in a humidified incubator for 24 hours. SMARTpool siRNA, or a scrambled siRNA control, was applied at 1 μM per well, incubated at 37°C and 5% CO_2 in a humidified incubator for 96 hours, and then infected and time-lapse–imaged as described above.

Secreted cytokine quantification

DuoSet ELISA Development kits from R&D Systems were used for all cytokine quantification and used according to the manufacturer's instructions. Secreted murine Ym1 was detected by sandwich ELISA using anti-Ym1 antibody (Abcam). Media supernatants from infected macrophages, treated with XMD17-109 or DMSO for 18 hours, were serially diluted before ELISA analysis and cytokine concentrations derived by reference to a standard curve.

Polarization assays

J774 macrophages were seeded at 0.2×10^6 cells per well in DMEM containing 10% heat-inactivated FBS and then stimulated with IL-4 (20 ng/ml) (ImmunoTools) or LPS (20 ng/ml) (Sigma-Aldrich) + 1000 IU IFN-γ (ImmunoTools), in the presence or absence of 1 μM XMD17-109. After 24 hours, the cells were placed on ice and stained for viability and macrophage activation markers (LIVE/DEAD Aqua Thermo, CD11b-BV605 BD, MGL-PE BioLegend, and CD86-FITC BD). Events were acquired using an Attune flow cytometer, and data were analyzed using FlowJo 8.7.

Statistical analysis

Statistical analysis was performed using a combination of Microsoft Excel, GraphPad Prism, MaxQuant (mass spectrometry tools), and the statistical program R, together with the online software DAVID

(Database for Annotation, Visualization and Integrated Discovery) to detect significant enrichment of gene ontology clusters (*29*).

Zebrafish

Animal work was carried out per guidelines and legislation set out in UK law in the Animals (Scientific Procedures) Act 1986, under Project License PPL 40/3574. Ethical approval was granted by the University of Sheffield Local Ethical Review Panel. We used the Nacre as our wild-type strain. We used the macrophage Tg(mpeg1:mCherryCAAX)sh378 fluorescent transgenic zebrafish line (*6*). Zebrafish strains were maintained according to the standard protocols. Adult fish were maintained on a 14:10-hour light/dark cycle at 28°C in UK Home Office–approved facilities in the Bateson Centre aquaria at the University of Sheffield. Zebrafish were infected as described previously (*6*) with 500 colony forming units of *Cryptococcus* strain KN99-GFP. For time-lapse imaging, zebrafish larvae were mounted in 0.8% low–melting point agarose in E3 containing tricaine (0.168 mg/ml). Images were captured with CFI Plan Apochromat λ [20×; numerical aperture (NA), 0.75 objective lens; 10 *z*-sections 2.5 μm apart], with Perfect Focus system, every 2 min for 12 hours. For co-infection studies, we used H99-GFP (*27*) and H99-dsRed (*30*). For fungal burden and dissemination imaging, zebrafish were imaged in 96-well plates using Nikon Ti-E with a CFI Plan Achromat UW (2×; NA, 0.06 objective lens), using Intensilight fluorescent illumination with ET/sputtered series fluorescent filters 49002 (Chroma). Images were captured with Neo sCMOS (Andor) and NIS Elements (Nikon). Images were exported as tif files, and further analysis was performed in ImageJ (*31*), as described previously (*6*).

SUPPLEMENTARY MATERIALS

Supplementary material for this article is available at http://advances.sciencemag.org/cgi/content/full/3/8/e1700898/DC1

table S1. Screened inhibitors of macrophage-expressed kinases.

fig. S1. Pharmacological inhibition of the MEK5/ERK5 signaling pathway does not alter cryptococcal growth in vitro.

fig. S2. Quantification of ERK5 depletion in macrophages.

movie S1. Example time-lapse movie showing vomocytosis from J774 cells infected with H99-GFP cryptococci and treated with DMSO (control).

movie S2. Example time-lapse movie showing vomocytosis from J774 cells infected with H99-GFP cryptococci and treated with 1 μM XMD17-109.

REFERENCES AND NOTES

1. M. Alvarez, A. Casadevall, Phagosome extrusion and host-cell survival after *Cryptococcus neoformans* phagocytosis by macrophages. *Curr. Biol.* **16**, 2161–2165 (2006).
2. H. Ma, J. E. Croudace, D. A. Lammas, R. C. May, Expulsion of live pathogenic yeast by macrophages. *Curr. Biol.* **16**, 2156–2160 (2006).
3. L. M. Smith, R. C. May, Mechanisms of microbial escape from phagocyte killing. *Biochem. Soc. Trans.* **41**, 475–490 (2013).
4. A. M. Nicola, E. J. Robertson, P. Albuquerque, L. da Silveira Derengowski, A. Casadevall, Nonlytic exocytosis of *Cryptococcus neoformans* from macrophages occurs in vivo and is influenced by phagosomal pH. *MBio* **2**, e00167-11 (2011).
5. S. A. Johnston, K. Voelz, R. C. May, *Cryptococcus neoformans* thermotolerance to avian body temperature is sufficient for extracellular growth but not intracellular survival in macrophages. *Sci. Rep.* **6**, 20977 (2016).
6. A. Bojarczuk, K. A. Miller, R. Hotham, A. Lewis, N. V. Ogryzko, A. A. Kamuyango, H. Frost, R. H. Gibson, E. Stillman, R. C. May, S. A. Renshaw, S. A. Johnston, *Cryptococcus neoformans* intracellular proliferation and capsule size determines early macrophage control of infection. *Sci. Rep.* **6**, 21489 (2016).
7. M. Carnell, T. Zech, S. D. Calaminus, S. Ura, M. Hagedorn, S. A. Johnston, R. C. May, T. Soldati, L. M. Machesky, R. H. Insall, Actin polymerization driven by WASH causes V-ATPase retrieval and vesicle neutralization before exocytosis. *J. Cell Biol.* **193**, 831–839 (2011).
8. J. Bain, L. Plater, M. Elliott, N. Shpiro, C. J. Hastie, H. Mclauchlan, I. Klevernic, J. S. C. Arthur, D. R. Alessi, P. Cohen, The selectivity of protein kinase inhibitors: A further update. *Biochem. J.* **408**, 297–315 (2007).
9. X. Deng, N. Dzamko, A. Prescott, P. Davies, Q. Liu, Q. Yang, J.-D. Lee, M. P. Patricelli, T. K. Nomanbhoy, D. R. Alessi, N. S. Gray, Characterization of a selective inhibitor of the Parkinson's disease kinase LRRK2. *Nat. Chem. Biol.* **7**, 203–205 (2011).
10. B. Seashore-Ludlow, M. G. Rees, J. H. Cheah, M. Cokol, E. V. Price, M. E. Coletti, V. Jones, N. E. Bodycombe, C. K. Soule, J. Gould, B. Alexander, A. Li, P. Montgomery, M. J. Wawer, N. Kuru, J. D. Kotz, C. S.-Y. Hon, B. Munoz, T. Liefeld, V. Dančík, J. A. Bittker, M. Palmer, J. E. Bradner, A. F. Shamji, P. A. Clemons, S. L. Schreiber, Harnessing connectivity in a large-scale small-molecule sensitivity dataset. *Cancer Discov.* **5**, 1210–1223 (2015).
11. N. Weygant, D. Qu, W. L. Berry, R. May, P. Chandrakesan, D. B. Owen, S. M. Sureban, N. Ali, R. Janknecht, C. W. Houchen, Small molecule kinase inhibitor LRRK2-IN-1 demonstrates potent activity against colorectal and pancreatic cancer through inhibition of doublecortin-like kinase 1. *Mol. Cancer* **13**, 103 (2014).
12. J. M. Elkins, J. Wang, X. Deng, M. J. Pattison, J. S. C. Arthur, T. Erazo, N. Gomez, J. M. Lizcano, N. S. Gray, S. Knapp, X-ray crystal structure of ERK5 (MAPK7) in complex with a specific inhibitor. *J. Med. Chem.* **56**, 4413–4421 (2013).
13. P. Ciceri, S. Müller, A. O'Mahony, O. Fedorov, P. Filippakopoulos, J. P. Hunt, E. A. Lasater, G. Pallares, S. Picaud, C. Wells, S. Martin, L. M. Wodicka, N. P. Shah, D. K. Treiber, S. Knapp, Dual kinase-bromodomain inhibitors for rationally designed polypharmacology. *Nat. Chem. Biol.* **10**, 305–312 (2014).
14. H. G. Choi, J. Zhang, X. Deng, J. M. Hatcher, M. P. Patricelli, Z. Zhao, D. R. Alessi, N. S. Gray, Brain penetrant LRRK2 inhibitor. *ACS Med. Chem. Lett.* **3**, 658–662 (2012).
15. B. A. Drew, M. E. Burow, B. S. Beckman, MEK5/ERK5 pathway: The first fifteen years. *Biochim. Biophys. Acta* **1825**, 37–48 (2012).
16. S. Amano, Y.-T. Chang, Y. Fukui, ERK5 activation is essential for osteoclast differentiation. *PLOS ONE* **10**, e0125054 (2015).
17. E. J. Carter, R. A. Cosgrove, I. Gonzalez, J. H. Eisemann, F. A. Lovett, L. J. Cobb, J. M. Pell, MEK5 and ERK5 are mediators of the pro-myogenic actions of IGF-2. *J. Cell Sci.* **122**, 3104–3112 (2009).
18. H.-S. Suh, M. Cosenza-Nashat, N. Choi, M.-L. Zhao, J.-F. Li, J. W. Pollard, R. L. Jirtle, H. Goldstein, S. C. Lee, Insulin-like growth factor 2 receptor is an IFNγ-inducible microglial protein that facilitates intracellular HIV replication: Implications for HIV-induced neurocognitive disorders. *Am. J. Pathol.* **177**, 2446–2458 (2010).
19. P. J. Murray, J. E. Allen, S. K. Biswas, E. A. Fisher, D. W. Gilroy, S. Goerdt, S. Gordon, J. A. Hamilton, L. B. Ivashkiv, T. Lawrence, M. Locati, A. Mantovani, F. O. Martinez, J.-L. Mege, D. M. Mosser, G. Natoli, J. P. Saeij, J. L. Schultze, K. A. Shirey, A. Sica, J. Suttles, I. Udalova, J. A. van Ginderachter, S. N. Vogel, T. A. Wynn, Macrophage activation and polarization: Nomenclature and experimental guidelines. *Immunity* **41**, 14–20 (2014).
20. K. Voelz, D. A. Lammas, R. C. May, Cytokine signaling regulates the outcome of intracellular macrophage parasitism by *Cryptococcus neoformans*. *Infect. Immun.* **77**, 3450–3457 (2009).
21. J. C. Barros, C. J. Marshall, Activation of either ERK1/2 or ERK5 MAP kinase pathways can lead to disruption of the actin cytoskeleton. *J. Cell Sci.* **118**, 1663–1671 (2005).
22. D. Spiering, M. Schmolke, N. Ohnesorge, M. Schmidt, M. Goebeler, J. Wegener, V. Wixler, S. Ludwig, MEK5/ERK5 signaling modulates endothelial cell migration and focal contact turnover. *J. Biol. Chem.* **284**, 24972–24980 (2009).
23. S. A. Johnston, R. C. May, The human fungal pathogen *Cryptococcus neoformans* escapes macrophages by a phagosome emptying mechanism that is inhibited by Arp2/3 complex-mediated actin polymerisation. *PLOS Pathog.* **6**, e1001041 (2010).
24. J. L. Tenor, S. H. Oehlers, J. L. Yang, D. M. Tobin, J. R. Perfect, Live imaging of host-parasite interactions in a zebrafish infection model reveals cryptococcal determinants of virulence and central nervous system invasion. *MBio* **6**, e01425-15 (2015).
25. C. Charlier, K. Nielsen, S. Daou, M. Brigitte, F. Chretien, F. Dromer, Evidence of a role for monocytes in dissemination and brain invasion by *Cryptococcus neoformans*. *Infect. Immun.* **77**, 120–127 (2009).
26. F. Qiu, L. Yang, W. Fang, Y. Li, R. Yang, X. Yang, J. Deng, B. Huang, C. Xie, Y. Zhou, J. Lu, A functional polymorphism in the promoter of *ERK5* gene interacts with tobacco smoking to increase the risk of lung cancer in Chinese populations. *Mutagenesis* **28**, 561–567 (2013).
27. K. Voelz, S. A. Johnston, J. C. Rutherford, R. C. May, Automated analysis of cryptococcal macrophage parasitism using GFP-tagged cryptococci. *PLOS ONE* **5**, e15968 (2010).
28. K. G. Finegan, X. Wang, E.-J. Lee, A. C. Robinson, C. Tournier, Regulation of neuronal survival by the extracellular signal-regulated protein kinase 5. *Cell Death Differ.* **16**, 674–683 (2009).
29. D. W. Huang, B. T. Sherman, Q. Tan, J. Kir, D. Liu, D. Bryant, Y. Guo, R. Stephens, M. W. Baseler, H. C. Lane, R. A. Lempicki, DAVID Bioinformatics Resources: Expanded annotation database and novel algorithms to better extract biology from large gene lists. *Nucleic Acids Res.* **35**, W169–W175 (2007).
30. A. Idnurm, S. S. Giles, J. R. Perfect, J. Heitman, Peroxisome function regulates growth on glucose in the basidiomycete fungus *Cryptococcus neoformans*. *Eukaryot. Cell* **6**, 60–72 (2007).
31. C. A. Schneider, W. S. Rasband, K. W. Eliceiri, NIH Image to ImageJ: 25 years of image analysis. *Nat. Methods* **9**, 671–675 (2012).

Acknowledgments: We thank the Bateson Centre aquaria staff at the University of Sheffield for their assistance with zebrafish husbandry. **Funding:** A.S.G., P.I.S., and R.C.M. are supported by project MitoFun, funded by the European Research Council under the European Union's Seventh Framework Programme (FP/2007-2013)/ERC grant agreement no. 614562 and by a Wolfson Research Merit Award from the Royal Society (to R.C.M.), a Biotechnology and Biological Sciences Research Council Midlands Integrative Biosciences Training Partnership Studentship (to A.S.G.), and a scholarship from the Darwin Trust of Edinburgh (to P.I.S.). S.A.J. and A.B. were supported by Medical Research Council and Department for International Development Career Development Award Fellowship (MR/J009156/1). S.A.J. was additionally supported by a Krebs Institute Fellowship, the Medical Research Foundation (grant R/140419), and the Medical Research Council Center (grant G0700091). R.H. was supported by a Colin Beattie Biomedical Science scholarship. A.R.S. was supported by a scholarship from the Higher Committee for Education Development in Iraq. E.G. was supported by a Marie Curie Research Fellowship, and C.T. is supported by a grant from Worldwide Cancer Research. G.V.V. is supported by a postdoctoral grant from the Flemish Research Foundation. D.R.A. acknowledges funding from the UK Medical Research Council (grant number MC-UU_1201612). **Author contributions:** A.S.G., P.I.S., and R.C.M. devised and led this project. A.S.G., P.I.S., and P.S.-C. conducted most of the in vitro experimental work and analyzed the data. A.B., R.H., and S.A.J. conducted and analyzed the zebrafish experiments. A.R.S., N.S.G., D.R.A., A.H., G.V.V., and D.L.C. provided the reagents, advice, and unpublished data to support this project. A.S.G. conducted the work on ERK5 knockout mouse material in collaboration with E.G. and C.T. All authors read and commented on the manuscript. **Competing interests:** N.S.G. is an author on a patent application related to this work filed by the Dana-Farber Cancer Institute (international application no. PCT/US2010/000050; filed 6 January 2010). N.S.G. is a scientific founder and equity holder in Gatekeeper, Syros, Petra, and C4 Pharmaceuticals. All other authors declare that they have no competing interests. **Data and materials availability:** All data needed to evaluate the conclusions in the paper are present in the paper and/or the Supplementary Materials. Additional data related to this paper may be requested from the authors.

Submitted 23 March 2017
Accepted 24 July 2017
Published 16 August 2017
10.1126/sciadv.1700898

Citation: A. S. Gilbert, P. I. Seoane, P. Sephton-Clark, A. Bojarczuk, R. Hotham, E. Giurisato, A. R. Sarhan, A. Hillen, G. V. Velde, N. S. Gray, D. R. Alessi, D. L. Cunningham, C. Tournier, S. A. Johnston, R. C. May, Vomocytosis of live pathogens from macrophages is regulated by the atypical MAP kinase ERK5. *Sci. Adv.* **3**, e1700898 (2017).

Science Advances

Vomocytosis of live pathogens from macrophages is regulated by the atypical MAP kinase ERK5

Andrew S. Gilbert, Paula I. Seoane, Poppy Sephton-Clark, Aleksandra Bojarczuk, Richard Hotham, Emanuele Giurisato, Adil R. Sarhan, Amy Hillen, Greetje Vande Velde, Nathanael S. Gray, Dario R. Alessi, Debbie L. Cunningham, Cathy Tournier, Simon A. Johnston and Robin C. May

Sci Adv **3** (8), e1700898.
DOI: 10.1126/sciadv.1700898